Supporting Information

Lohr et al. 10.1073/pnas.1402134111

SI Materials and Methods

Generation of Transgenic Mice. BAC RP23-292H20 contains the entire vesicular monoamine transporter 2 (VMAT2) (*Slc18a2*) locus (35 kb), 100 kb upstream and 60 kb downstream. BAC DNA was introduced into C57Bl/6 and FVB embryos using pronuclear injection. A total of 12 lines were generated (8 FVB and 4 C57Bl/6), 5 of which showed functional elevated VMAT2 as confirmed by Western blot and vesicular uptake. Positive founders were identified by PCR genotyping using primers against BAC sequences and confirmed by Southern blotting. Line 1 was designated VMAT2-HI.

Western Blotting and Immunohistochemistry Antibodies. Rabbit polyclonal anti-VMAT2 serum was raised against a peptide in the C-terminal region of mouse VMAT2 (CTQNNVQPYPVGDDEESESD) by Covance Custom Immunology Services. Primary antibodies used were as follows: polyclonal rabbit anti-VMAT2 serum (1:20,000), rat anti-DAT (1:1,000; Millipore), rabbit anti-TH (1:1,000; Millipore), and mouse anti–β-actin (1:5,000; Sigma). The appropriate HRP-linked secondary antibodies (1:5000; Jackson ImmunoResearch) were used. For immunohistochemistry (IHC), primary antibodies used were as follows: polyclonal rabbit anti-VMAT2 serum (1:50,000), rat anti-DAT (1:1,000; Millipore), or rabbit anti-TH (1:1,000; Millipore). The appropriate biotinylated secondary antibodies (1:200; Jackson ImmunoResearch) were used.

Electron Microscopy. Following perfusion of mice with 4% (wt/vol) paraformaldehyde (PFA) and 0.2% glutaraldehyde and overnight immersion of brains in 4% PFA at 4 °C, 50-μm sections were cut with a vibratome. Preembedding immunogold electron microscopy was performed as described previously, without a permeabilization step and with one round of secondary antibody incubation and silver enhancement (1). Following incubation with rabbit anti-TH antibody, tissue was incubated with ultrasmall colloidal gold-conjugated goat anti-rabbit antibody (Aurion).

Fast-Scan Cyclic Voltammetry in Striatal Slice. Application of waveform, stimulus, and current monitoring was controlled by TarHeel CV [University of North Carolina (UNC)] using a custom potentiostat (UEI, UNC Electronics Shop). The waveform for dopamine detection consisted of a −0.4 V holding potential versus an Ag/AgCl (In Vivo Metric) reference electrode. The applied voltage ramp goes from −0.4 V to 1.0 V and back to -0.4 V at a rate of 600 V/s at 60 Hz.

No-Net Flux Microdialysis. After anesthetization with 2,2,2-tribromoethanol, the microdialysis probe was implanted into the caudoputamen [anteroposterior (AP) 0.6 mm, mediolateral (ML) 1.7 mm, and dorsoventral (DV) 4.5 mm from bregma] and perfused with artificial cerebrospinal fluid (aCSF) (0.6 μL/min) overnight. The next day, the probe was perfused with 0 nM, 2 nM, 10 nM, and 20 nM dopamine (C_{in}) in random order at 0.6 μL/min. Samples (C_{out}) were collected at 40-min intervals. Basal dopamine levels were determined by linear regression of the gain or loss of dopamine from the perfusate ($C_{in} - C_{out}$) versus C_{in}. The extraction fraction is the slope of the linear regression analysis. Neurotransmitters were identified by HPLC by matching retention time to that of known dopamine standards. Probe placement was verified after the experiment.

1. Yi H, Leunissen J, Shi G, Gutekunst C, Hersch S (2001) A novel procedure for preembedding double immunogold-silver labeling at the ultrastructural level. *J Histochem Cytochem* 49:279–284.

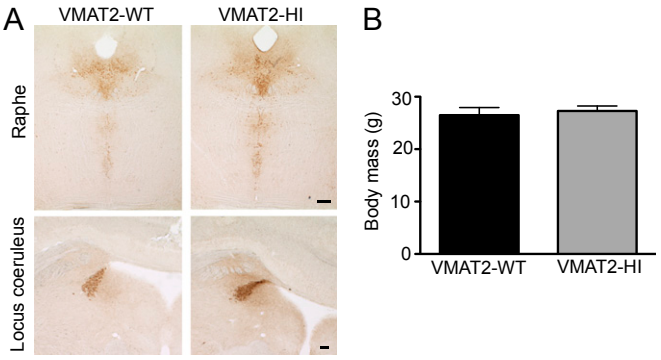

Fig. S1. VMAT2 overexpression in other brain regions and VMAT2-HI body mass. (*A*) VMAT2 overexpression has been confirmed both in the raphe and locus coeruleus in the VMAT2-HI mice. (Scale bars: 200 μm.) (*B*) No difference in body mass between VMAT2-HI and wild-type adult male mice ($n = 10$).

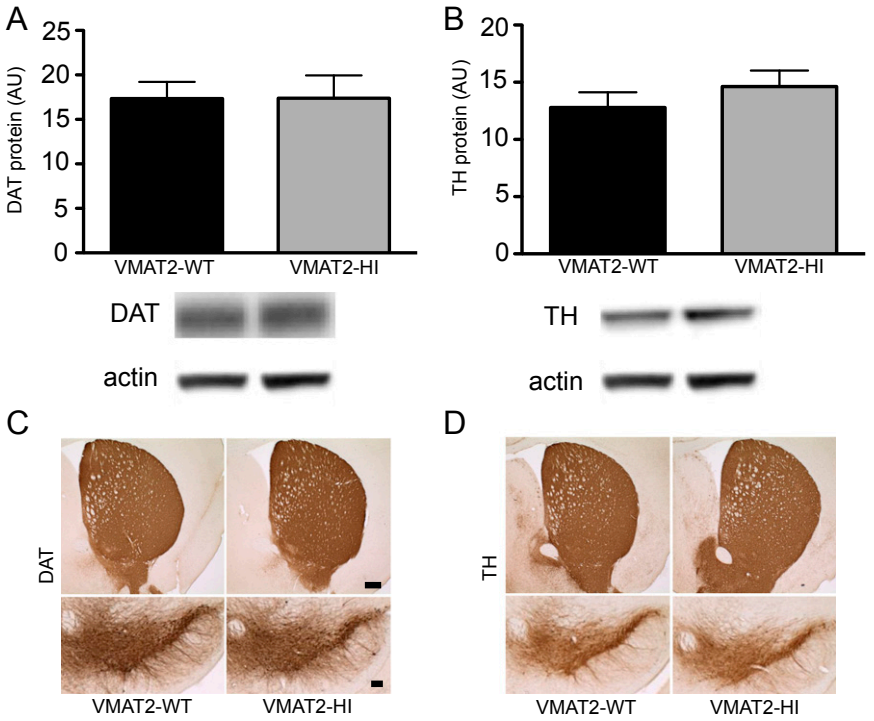

Fig. S2. VMAT2-HI mice show no changes to tyrosine hydroxylase (TH) and dopamine transporter (DAT) levels. No changes were observed in expression levels of other synaptic dopamine markers including DAT (*A* and *C*) and the TH (*B* and *D*) by immunochemistry (n = 12). (Scale bars: 200 μm.)

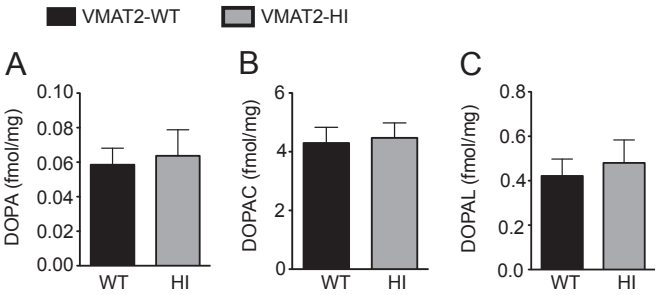

Fig. S3. VMAT2-HI mice show no changes to cytosolic dopamine metabolism as measured by HPLC. (*A*–*C*) No differences were seen in dopamine metabolites 3,4-dihydroxylphenylalanine (DOPA), 3,4-dihydroxyphenylacetic acid (DOPAC), and 3,4-dihydroxyphenylacetaldehyde (DOPAL) between wild-type and VMAT2-HI mice (n = 20–21).

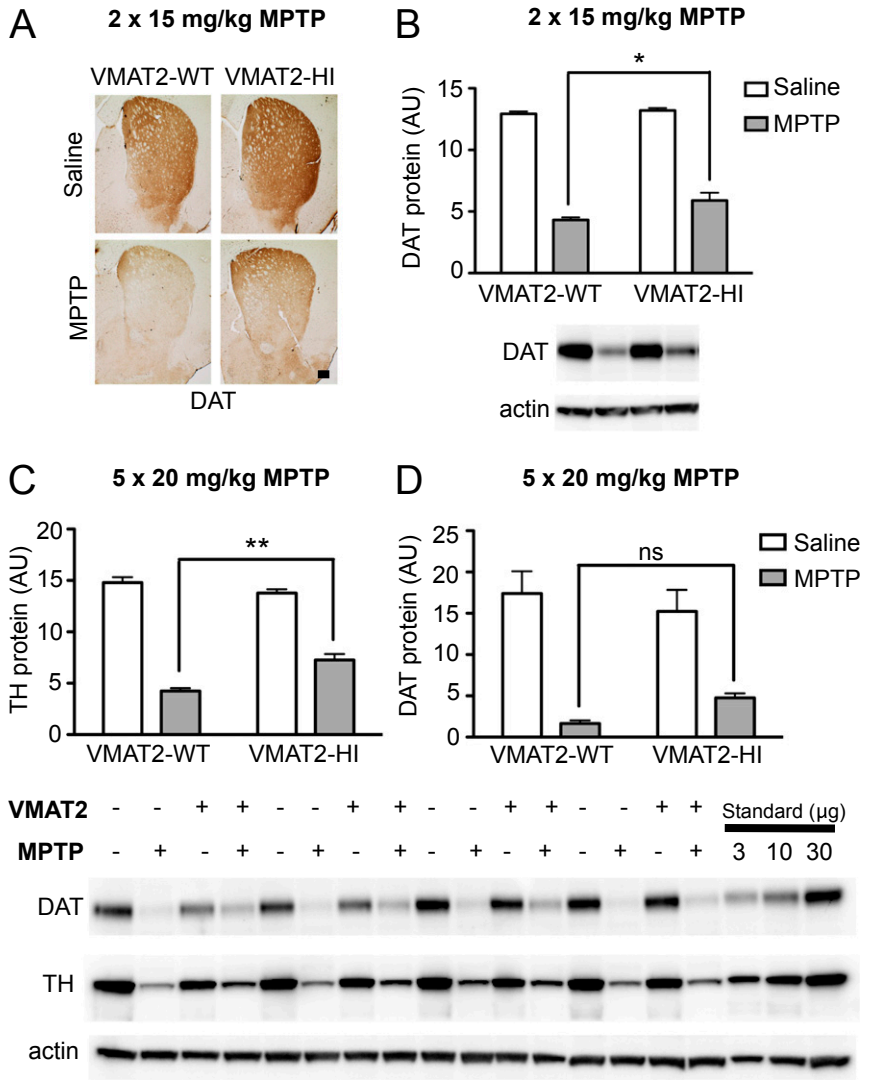

Fig. S4. Other measures of 1-methyl-4-phenyl-1,2,3,6-tetrahydropyridine (MPTP) protection in the VMAT2-HI mice. (*A* and *B*) VMAT2-HI mice also show significant protection from DAT loss in the striatum following a 2 × 15 mg/kg MPTP dose as shown by immunohistochemistry and measured by immunoblotting ($n = 4$). (Scale bar: 200 μm.) (*C* and *D*) VMAT2-HI mice show significant protection from striatal TH loss and a trend toward protection from striatal DAT loss following a 5 × 20 mg/kg MPTP dose ($n = 4$). Western blot of both genotypes (–, wild-type; +, VMAT2-HI) following MPTP treatment with codilutional standard of pooled control tissue used for quantification (3 μg, 10 μg, and 30 μg of protein).

Table S1. Unchanged behaviors in the VMAT2-HI mice

Behavior	Output	VMAT2-WT (avg ± SEM)	VMAT2-HI (avg ± SEM)	*P* value
Elevated plus maze ($n = 10$)	Open arm entries	6.5 ± 0.7	7.7 ± 2.4	> 0.05
Social odor discrimination ($n = 9$)	Time spent sniffing stranger (% of total investigation time)	68.3 ± 4.6	67.5 ± 4.1	> 0.05
Sleep latency ($n = 9$)	Latency to sleep (min)	23.5 ± 3.0	19.8 ± 3.8	> 0.05

VMAT2-HI mice show no significant changes in the listed behavioral assays.

Table S2. Other synaptic features are unchanged in VMAT2-HI mice

Measurement	VMAT2-WT (avg ± SEM)	VMAT2-HI (avg ± SEM)
Mitochondria area, nm^2	145,375 ± 22,254	119,364 ± 16,016
Synaptic cleft width, nm	20.74 ± 1.04	19.60 ± 1.05
Terminal area, nm^2	312,171 ± 36,223	362,890 ± 43,330
Vesicles per terminal	4.089 ± 0.37	4.517 ± 0.36

VMAT2-HI mice show no changes in mitochondrial size, synaptic cleft width, terminal area, and vesicle number as measured from immunogold electron micrographs in TH^+ striatal terminals.